



Chip-based molecularly imprinted monolithic capillary array columns coated GO/SiO₂ for selective extraction and sensitive determination of rhodamine B in chili powder



Haiyun Zhai^{a,*}, Lu Huang^a, Zuanguang Chen^b, Zihao Su^a, Kaisong Yuan^a, Guohuan Liang^a, Yufang Pan^a

^a College of Pharmacy, Guangdong Pharmaceutical University, Guangzhou 510006, China

^b School of Pharmaceutical Science, Sun Yat-sen University, Guangzhou 510006, China

ARTICLE INFO

Article history:

Received 26 December 2015

Received in revised form 19 July 2016

Accepted 20 July 2016

Available online 21 July 2016

Keywords:

Rhodamine B

Molecularly imprinted solid-phase extraction

Micro-fluidic chip

Monolithic array column

Chili powder

ABSTRACT

A novel solid-phase extraction chip embedded with array columns of molecularly imprinted polymer-coated silanized graphene oxide (GO/SiO₂-MISPE) was established to detect trace rhodamine B (RB) in chili powder. GO/SiO₂-MISPE monolithic columns for RB detection were prepared by optimizing the supporting substrate, template, and polymerizing monomer under mild water bath conditions. Adsorption capacity and specificity, which are critical properties for the application of the GO/SiO₂-MISPE monolithic column, were investigated. GO/SiO₂-MIP was examined by scanning electron microscopy (SEM) and Fourier transform-infrared spectroscopy. The recovery and the intraday and interday relative standard deviations for RB ranged from 83.7% to 88.4% and 2.5% to 4.0% and the enrichment factors were higher than 110-fold. The chip-based array columns effectively eliminated impurities in chili powder, indicating that the chip-based GO/SiO₂-MISPE method was reliable for RB detection in food samples using high-performance liquid chromatography. Accordingly, this method has direct applications for monitoring potentially harmful dyes in processed food.

© 2016 Elsevier Ltd. All rights reserved.

1. Introduction

The overuse of additives in foodstuffs, especially harmful dyes, is considered a great threat to human health. The water-soluble xanthene dye rhodamine B (RB, 9-(2-carboxyphenyl)-3,6-bis(diethylamino) xanthylium chloride) has previously been employed as a fluorescent dye to stain cells in laboratory applications (Longmire et al., 2008), as well as in the cosmetics, textiles, fireworks, and colored glass industries. In addition, RB has frequently been added to chili powder and chili oil as a colorant. However, it has potential toxic and carcinogenic effects, and it irritates the skin, eyes, and respiratory tract (International Agency for Research on Cancer, <http://www.iarc.fr/>). Various analytical methods have been adopted for RB determination, such as high-performance liquid chromatography (HPLC) (Tatebe et al., 2014) and capillary zone electrophoresis (Milanova, Chambers, Bahga, & Santiago, 2011). HPLC has good precision, high resolution, and a simple analysis procedure, and capillary zone electrophoresis is widely used owing to its speed, high separation efficiency, and low cost.

Molecularly imprinted polymers (MIPs), which are synthetic polymers characterized by high selectivity and specific recognition towards target analytes, are often coupled with solid-phase extraction (SPE) (Zhang, Zeng, Wang, & Chen, 2013). Molecularly imprinted solid-phase extraction (MISPE) is a widely employed procedure for sample clean-up within complicated matrixes. MISPE can be applied to analyte separation/preconcentration; additionally, it significantly reduces interference from impurities compared with other traditional SPE techniques (Olof, Kristina, John, Pradip, & Oliver, 2014). Considering the chemical stability and selectivity of polymers, MISPE monolithic columns are used in many fields, such as biological chemistry (Meng, Zhang, Bao, & Chen, 2015), food security (Lata, Sharma, Naik, Rajput, & Mann, 2015), and environmental pollution control (Wang, Xu, Fang, Zhang, & He, 2008).

In situ polymerization is an important and frequently used approach to prepare monolithic porous imprinting polymers. However, owing to a high diffusion barrier and poor site accessibility, the adsorption performances of traditional SPE techniques are limited. In order to address these problems, surface imprinting techniques, especially those involving nanomaterials, have been adopted to facilitate template molecule removal and enhance binding capacity (Li, Qi, & Ma, 2013). Additionally, various

* Corresponding author.

E-mail address: zhaihaiyun@126.com (H. Zhai).

nanosized materials have been used as substrates, including silica nanoparticles (Jackson et al., 2015), metal nanoparticles (Gao, Chen, & Jiang, 2013), quantum dot nanoparticles (Liu et al., 2013), Fe₃O₄ nanoparticles (Ning, Peng, Li, Chen, & Xiong, 2014), carbon nanotubes (Unsal, Soyak, & Tuzen, 2014), and graphene. As a promising self-supporting material with unique mechanical properties and a large surface area, graphene has provided a basis for the synthesis of functional materials, such as graphene oxide (GO) (Farid, Goudini, Piri, Zamani, & Saadati, 2016), reduced graphene oxide (Xiao, Zhang, & Liu, 2015), and functional graphene oxides (e.g., silanized graphene oxide, GO/SiO₂). Our previous work (Zhai et al., 2015) revealed that in situ polymerized MIPs coated with GO exhibit higher loading capacity and faster association kinetics than MIPs alone, leading to improved analyte detection sensitivity. In order to solve the problem of poor GO solubility, additional processing procedures such as silanization and sulfonation were introduced to improve mass transfer, increase the GO content in columns, and improve the capacity of array columns. As there were a number of hydroxy groups, the GO/SiO₂ substrate proved to be a more suitable composite than GO on the glass capillary inner wall and on the GO/SiO₂ surface (Duan et al., 2015).

In this study, highly selective RB-imprinted polymers coated on GO/SiO₂ surfaces were evaluated for MISPE and preconcentration. A combined chip with four columns of GO/SiO₂-MISPE was established to selectively enrich RB in chili powder samples further increase the enrichment capacity, and improve selection efficiency. The MIP columns were evaluated using analytical methods. In addition, an RB MIP monolithic capillary column without GO/SiO₂ was prepared for a comparative analysis. Under mild water-bath conditions, RB MIPs were prepared in a glass capillary column (10 cm × 500 µm, i.d.) by synthesizing the template (RB), monomer, porogen, cross-linker, and initiator. Several important parameters were optimized to improve the adsorption capacity, such as the template: monomer: cross-linker (T:M:C) ratio, porogen types, and eluent conditions. Finally, a good separation-preconcentration effect of RB in samples was achieved on the array chip. To our knowledge, the proposed method is the first application of chip-based GO/SiO₂ MISPE monolithic array columns to sensitively detect RB in chili powder.

2. Experimental

2.1. Materials and reagents

Methacrylic acid (MAA), graphite powder, RB, safranin T, polydimethylsiloxane (PDMS) and ethylene dimethacrylate (EDMA), curing agent (SYLGARD 184) and azobisisobutyronitrile (AIBN) were all purchased from Aladdin industrial corporation (Shanghai, China). All chemical reagents used in this study were of analytical reagent grade and from Guangzhou Chemical Reagents Co (China). Methanol was of HPLC-grade purchased from Merck Company (Germany) and the chili powder was purchased from a department store. The distilled water was supplied by Watsons and all samples were dissolved and filtered before injection.

2.2. Fabrication of the GO/SiO₂-MISPE monolithic capillary column

Silanized graphene oxide (GO/SiO₂) was synthesized by two steps. First, GO was synthesized from graphite powder according to a method reported by Hummers & Offeman (1958). Second, the GO surface was modified with 3-aminopropyltriethoxysilane (APTES), which provided a π - π interaction, to obtain GO/SiO₂ (Zeng, Zhou, Kong, Zhou, & Shi, 2015).

Using an in situ polymerization method, GO/SiO₂-MIPs were synthesized in a glass capillary. In short, GO/SiO₂ (5 mg) was

dispersed in porogen-containing methanol (0.5 mL), toluene (1.0 mL), and dodecanol (1.5 mL) for 0.5 h by ultrasonication. In the next step, the template RB (0.1 mmol) and polymerizing monomer MAA (0.4 mmol) were added. The crosslinker EDMA (3 mmol) and initiator AIBN (0.2 mmol) were added successively, while mechanically stirring the mixture for 0.5 h at room temperature (25 °C). To promote polymerization, the mixed solution was dissolved and degassed for a few minutes and then sucked into the glass capillary and initiated in a water bath at 60 °C for 4 h. At a rate of 0.1 mL min⁻¹, the synthetic RB-imprinted column was then washed with 2 mL of methanol-acetic acid (90:10, v/v) to eliminate the remaining template, until RB could not be detected by HPLC.

Non-imprinted polymers (GO/SiO₂-NIPs) were obtained in a similar manner, without the RB template. MIPs free of GO/SiO₂ were also prepared.

2.3. Preparation and construction of the PDMS-glass chip and chip-based MISPE monolithic columns

As described in our previous work (Zhai et al., 2014), the PDMS substrate and PDMS/glass chip were prepared using the molding method (Duffy, McDonald, Seubler, & Whitesides, 1998). The designed chip consisted of a platform (63 mm × 63 mm), four SPE channels (3.5 cm in length, 0.1 cm in width, 0.1 cm in height), and two ports (0.2 mm in diameter). Coupled with MISPE monolithic capillary columns (3.5 cm × 500 µm, i.d.), hollow SPE channels were bonded with epoxy glue and specific processing steps were performed as follows. First, a 3D stereogram layout of the microchannel network was designed using AutoCAD and the copper mold for the network was fabricated using an available merchant carving apparatus. Secondly, a mixture of PDMS elastomer and Sylgard 184 curing agent (10:1, w/w), i.e., a PDMS prepolymer, was degassed for 20 min to remove bubbles, poured into the copper mold, and solidified at 80 °C for 30 min. After completing the above process, the PDMS layer was removed from the mold using a clean scalpel. A PDMS chip substrate with microchannels was successfully prepared. Third, part of the SPE channel (approximately 3.3 cm) was cut off for use with the MISPE monolithic capillary columns after two holes of appropriate pore sizes were punched for input/output ports. Finally, the PDMS substrate and a glass cover plate (63 mm × 63 mm) with a thickness of 3.0 mm were placed in the oxygen plasma machine for surface modification for approximately 2 min, and were sealed together using external pressure. By bonding two layers using stress, the PDMS/glass chip was fabricated in an oven at 80 °C for 12 h. Consequently, the PDMS/glass chip with 4 integrated MISPE monolithic capillary array columns was prepared, as shown in Fig. 1.

2.4. Preparation and procedure for the determination of RB in chili powder samples

Chili powders (1.0 g) supplemented with RB standard solutions were dissolved by ultrasonic extraction with 4.0 mL of water and then centrifuged for 10 min (4000 rpm). After repeating these steps, the supernatant was collected and diluted to 8.0 mL with water. The spiked sample solutions at 0.01, 0.1, 1.0 µg mL⁻¹ were passed through chip-based MISPE monolithic array columns at a flow rate of 0.02 mL min⁻¹ after activation with 80 µL of methanol and water. After washing with 80 µL of toluene, the effluent was obtained by eluting the array chip with 80 µL of methanol-acetic acid (90:10, v/v) at a flow rate of 0.1 mL min⁻¹. Then, the evaporated residues were dissolved in an Eppendorf tube with 0.2 mL of water for the HPLC analysis. In addition, other 20 kinds of chili powders as real blank samples were tested following the same methods.

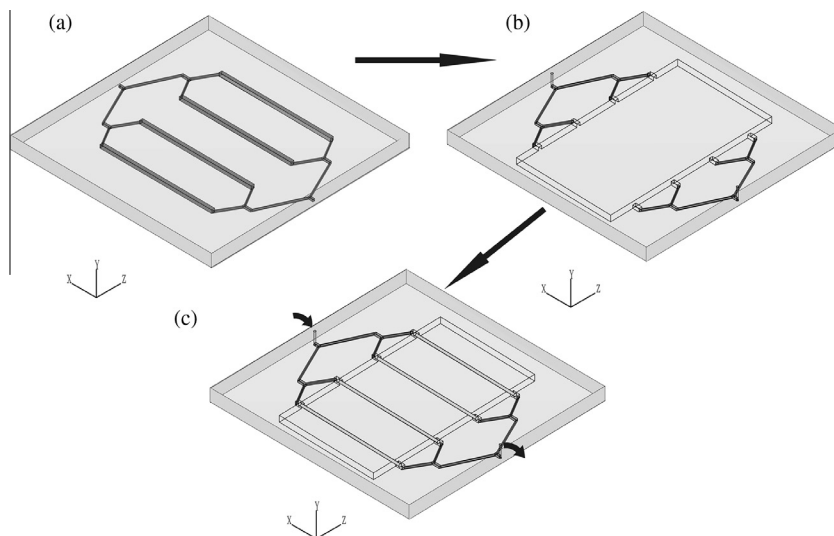


Fig. 1. Schematic illustration of the fabrication for MISPE-PDMS/glass chip: (a) PDMS/glass chip was fabricated; (b) part of SPE channel in PDMS layer was cut off; (c) MISPE monolithic capillary columns were coupled with PDMS/glass chip to form the final chip.

2.5. HPLC conditions

The chromatographic column for separation was Ecosil EPS-C₁₈ column (250 mm × 4.6 mm, 5 μm), and the mobile phase was methanol-water (80:20, v/v) with a flow rate of 1.0 mL min⁻¹. Analytical process was carried out on a Shimadzu LC-10A HPLC system (Japan) coupled with a RF-10AXL detector. The injection volume was 20 μL and excitation wavelength and emission wavelength were set as 530 nm and 590 nm, respectively.

3. Results and discussion

3.1. Synthesis and morphology of the GO/SiO₂-MISPE monolithic capillary column

In this study, the proper porogen was an essential factor in the molecular imprinting process; it was used for the polymerization reaction and its polarity significantly influenced the strength of non-covalent polymer interactions (Castro López et al., 2012). Additionally, its properties and dosage determined the pore size and shape of molecular imprinting materials. Various nonpolar or aprotic solvents, such as acetonitrile, polyethylene glycol, ethanol-water, acetonitrile-toluene, and methanol-toluene-dodecanol, were tested. GO/SiO₂-MIPs were homogeneous and permeable at a flow rate of 0.15 mL min⁻¹ when methanol-toluene-dodecanol was used as the porogen. Since slightly polar solvents did not effectively dissolve MIPs, methanol was added to the porogen to improve GO/SiO₂ solubility.

The molar ratio of T:M:C is another important parameter determining the loading capability of the GO/SiO₂-MISPE monolithic column. To optimize the T:M:C ratio, 200 μL of 5.0 μg mL⁻¹ RB standard solution was loaded into the column and the recovery (91.5%) was calculated as the proportion of RB injected into the GO/SiO₂-MISPE column. The optimal specific affinity was observed when T:M:C reached 1:4:20 (Table S₁).

To obtain a stable and homogeneous polymer structure, alkaline templates, such as RB (Fig. S₁), tend to be optimally paired with acidic monomer (MAA) to form complex, serving as a polymerizing monomer based on the Lewis acid-base theory. As shown in Fig. 2a and b, different porogens on the monolithic column were investigated based on scanning electron microscope (SEM) images, such as acetonitrile and a mixture of toluene, methanol, and

dodecanol. The monolithic column prepared with acetonitrile exhibited an irregular gap and an unhomogeneous structure, which led to nonspecific MIP absorption. The column prepared with the porogen mixture of toluene and dodecanol exhibited a well-formed and dense structure. SEM images of MIPs and GO/SiO₂-MIPs are presented in Fig. 2c and d, and SEM images of GO/SiO₂-MIPs at 20,000× magnification are shown in Fig. 2e. The compact network skeleton and homogeneous pores of the GO/SiO₂-MISPE were apparent, as presented in Fig. 2e. With the optimal pore size, the monolithic column was indeed able to ensure favorable transport on a micro pump at a flow rate of 0.15 mL min⁻¹. Additionally, the chemical structures of crude GO, GO/SiO₂, and GO/SiO₂-MIPs were characterized by Fourier transform-infrared spectroscopy (FT-IR) (Fig. 3). According to the FT-IR spectrum of GO (Fig. 3a), the peak at 1727 cm⁻¹ (C=O) corresponded to a particular stretching vibration peak, which consistent with —COOH and —OH groups. When ATPS (3-aminopropyltriethoxysilane) reacted with protonated functional groups via covalent bonds, the peak of C=O on GO would weaken. However, 1090 cm⁻¹ (C—O—Si) on GO/SiO₂ (Fig. 3b) appeared as an asymmetrical stretching vibration peak. Additionally, 951 cm⁻¹, 800 cm⁻¹, and 474 cm⁻¹ peaks belonged to symmetrical, asymmetrical, and flexural vibrations of Si—O—Si, respectively. The FT-IR spectrum of GO/SiO₂-MIPs (Fig. 3c) displayed well-defined characteristic peaks of MIPs at 1729 cm⁻¹ (C=O), 1264 cm⁻¹ (C—O), and 1149 cm⁻¹ (C—O), which were attributed to the C=O stretching vibration, C—O symmetric stretching vibration, and C—O antisymmetric stretching vibration. In fact, the high peak intensities at 1729 cm⁻¹ and 1149 cm⁻¹ strongly indicated the presence of MAA in MIPs and absorption peaks of GO/SiO₂ at 951 cm⁻¹, 800 cm⁻¹, and 474 cm⁻¹ were also included. The process of GO/SiO₂ bonding to MIPs confirmed that GO/SiO₂-MIPs were successfully synthesized.

3.2. Capacity and selectivity of the GO/SiO₂-MISPE monolithic capillary column

Using breakthrough curves, the adsorption capacity of the GO/SiO₂-MISPE column was investigated based on adsorption volume, which was closely associated with extraction efficiency. To this end, an 8.0-cm GO/SiO₂-MIP column (weight, 3.25 mg) and another 8.0-cm GO/SiO₂-NIP column (weight, 8.76 mg) were studied. There were more RB-imprinted adsorption sites in the MISPE column

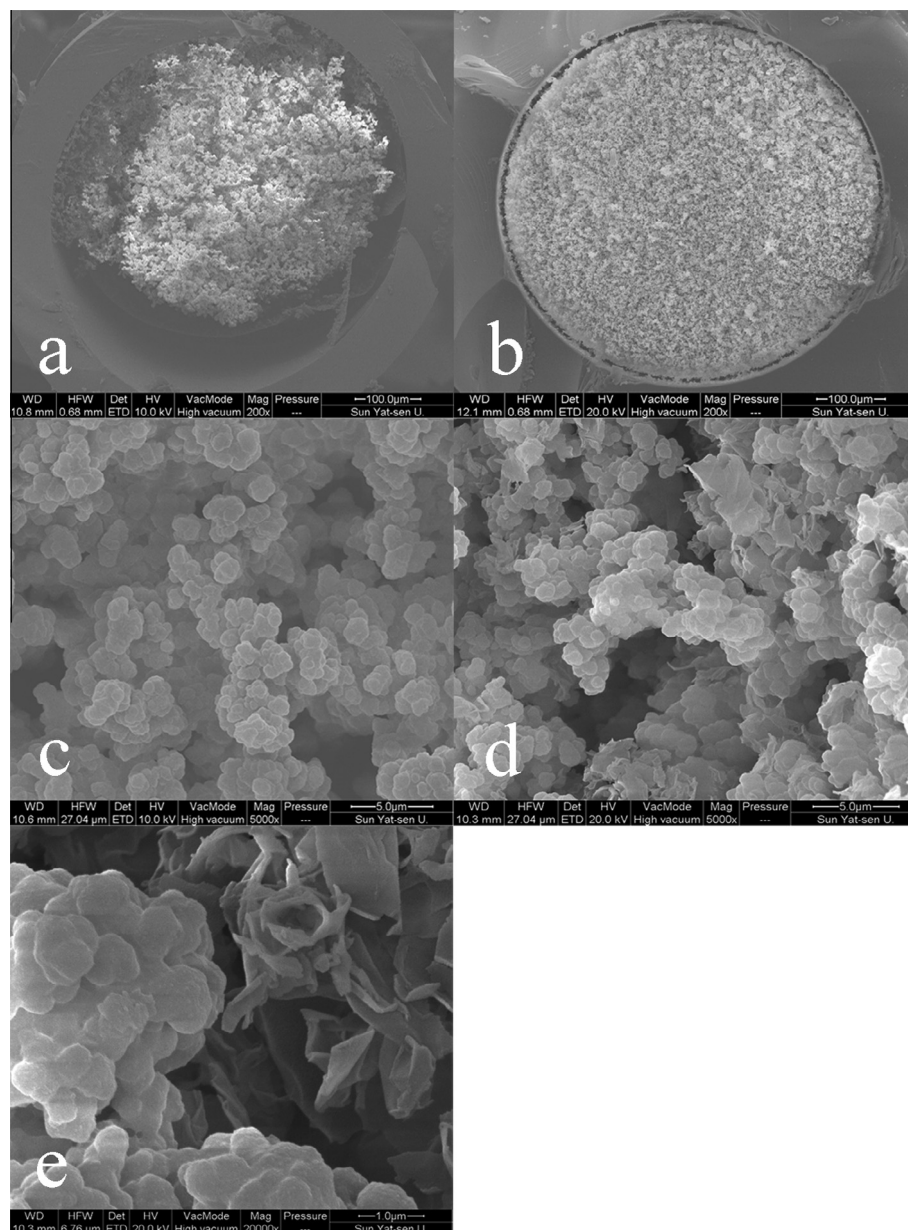


Fig. 2. SEM images of (a) the column prepared with acetonitrile, (b) the column prepared with methanol-toluene-dodecanol, (c) 5000 folds of MIPs, (d) 5000 folds of GO/SiO₂-MIPs and (e) the magnification is 20,000 folds of GO/SiO₂-MIPs.

than in the NISPE column after washing with suitable eluent, resulting in different amounts of GO/SiO₂-MIPs and GO/SiO₂-NIPs.

The adsorption process was carried out by extraction on the GO/SiO₂-MISPE column, loading 10.0 μg mL⁻¹ RB standard solution into the column at a moderate flow rate of 0.02 mL min⁻¹, and then collecting a series of effluents at various volumes before the HPLC analysis. Breakthrough curves of GO/SiO₂-MIP and GO/SiO₂-NIP monolithic columns were plotted according to injection volume and sample content (RB leakage). Initially, RB was highly retained when passing through the unsaturated monolithic column, which led to low sample content, as shown in Fig. 4. As the injection volume increased, the inner capacity of the monolithic column gradually reached saturation, until excess analyte (RB) flowed out from the column and nearly reached the injection concentration. After calculations and data analysis, the capacities of GO/SiO₂-MIPs and GO/SiO₂-NIPs were estimated as 1.994 μg mg⁻¹ and 0.282 μg mg⁻¹, which suggested that GO/SiO₂-MISPE exhibited a higher affinity for adsorption sites than GO/SiO₂-NISPE alone.

Accordingly, an 8.0-cm GO/SiO₂-MIP column (weight, 3.25 mg) and another 8.0-cm MIP column (weight, 3.12 mg) were tested to verify that GO/SiO₂ coated with MIPs could increase the column capacity. Based on the observed capacities of GO/SiO₂-MIPs (1.994 μg mg⁻¹) and MIPs (1.756 μg mg⁻¹), GO/SiO₂-MISPE had a higher adsorption capacity when compared with MISPE. The addition of nanomaterials (GO/SiO₂) for support, providing a large surface area and stable spatial structure, may have provided more binding sites on the surface of MIPs, improved the efficiency of mass transfer, and significantly increased polymer stability.

To further characterize the column specificity, the selective properties of the column towards RB and various compounds with similar structures, e.g., safranin T, phloxine B, and rose bengal, were investigated. Using the same GO/SiO₂-MISPE monolithic column, the adsorption capacities of RB, safranin T, phloxine B, and rose bengal imprinted columns were 1.994 μg mg⁻¹, 0.967 μg mg⁻¹, 0.906 μg mg⁻¹, and 0.725 μg mg⁻¹, indicating higher selectivity to RB, as shown in Fig. S2. Based on the parameters

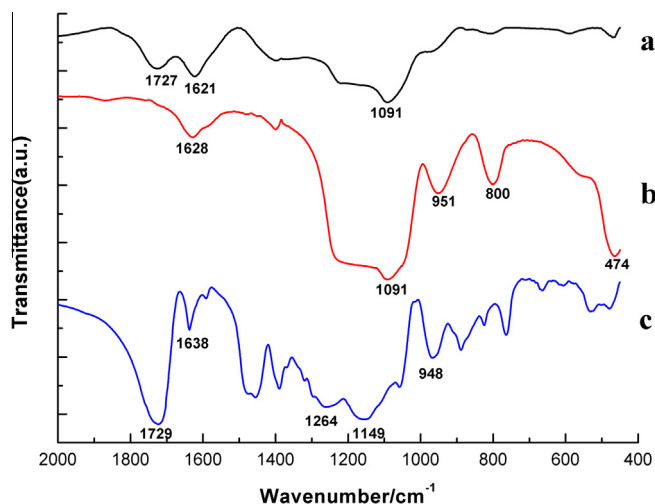


Fig. 3. FT-IR spectra of (a) GO, (b) GO/SiO₂, (c) GO/SiO₂-MIPs.

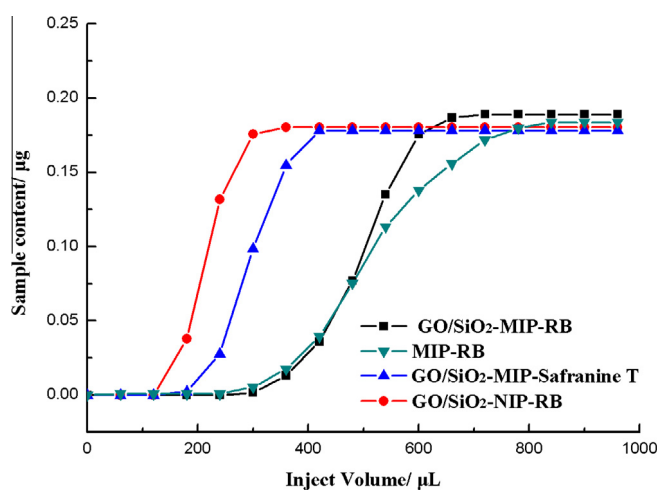


Fig. 4. Breakthrough curves of RB on GO/SiO₂-MIPs, MIPs and GO/SiO₂-MIPs column and breakthrough curves of safranin T on GO/SiO₂-MIPs column. Loading concentration: 10.0 μg mL⁻¹; Sample flow rate: 0.02 mL min⁻¹.

summarized above, the imprinting factor (IF) was calculated as 7.07 for GO/SiO₂-MIPs of RB using the following equation: $IF = Q_{MIP}/Q_{NIP}$, where Q_{MIP} is adsorption capacity of MISPE and Q_{NIP} is the adsorption capacity of NISPE, as shown in Table S₂. The IF estimates revealed good selectivity of the GO/SiO₂-MISPE monolithic column for RB when compared with other similar compounds.

3.3. Selection of an eluent and washing solvent

To test the imprinting effect and applicability of MIPs for the separation and detection of target analytes, the eluent and washing solvent were optimized to minimize interference. Compared with other low-polar solvents (cyclohexane and chloroform), toluene was able to clean up most of the impurities more effectively in the column, whereas chloroform and cyclohexane were ineffective due to poor retention properties towards the target analyte. Therefore, toluene was chosen as a suitable washing solvent, consistent with previous results (Yuan et al., 2015). To optimize the eluent and its dosage, 20 or 40 μL of the solvent with various ratios of methanol–acetic acid (100:0, 90:10, 80:20, 70:30, v/v) was tested. By loading 20 μL of 5.0 μg mL⁻¹ RB standard solution onto the column, the recovery of RB reached 91.5% using 40 μL of methanol–acetic acid (90:10, v/v) (Table S₃).

3.4. Method validation

The regression of RB concentration and peak areas indicated linearity under optimized experimental conditions. With a correlation coefficient of 0.9996, the linear regression equation was $A = 1.39 \times 10^6 C + 465.61$ over 0.001–20.0 μg mL⁻¹. At three different spiked concentration levels (0.01, 0.1, 1.0 mL⁻¹), recoveries of 83.7% to 88.4% were achieved for chili powder, while intra-day and inter-day relative standard deviations (RSD) were in the range of 2.5% to 4.0%, as shown in Table 1. Accordingly, the method demonstrated high precision for low concentrations with a limit of detection (LOD, S/N = 3) and limit of quantitation (LOQ, S/N = 10) of 0.05 ng mL⁻¹ and 0.16 ng mL⁻¹, respectively. These results indicated that this method was more sensitive than other HPLC (Tatebe et al., 2014) and UV–vis spectrophotometry (0.80 μg L⁻¹) (Unsal et al., 2014) methods, and this inference was supported by the lower LOD (0.40 ng g⁻¹). To verify the utility of this method for real samples, 20 different batches of chili powder were tested, and 2 spices were identified that could determine the occurrence of RB (Table S₄).

3.5. Enrichment and impurity removal

To verify the benefits of the method with respect to enrichment and impurity removal for trace sample detection, a spiked chili powder sample with 10.0 ng mL⁻¹ RB was applied to the array chip; the results are summarized in Fig. 5. In brief, 8.0 mL of the chili powder sample solution containing 10.0 ng mL⁻¹ RB was loaded onto the chip-based GO/SiO₂-MISPE array columns and then washed with 80 μL of toluene and eluted with methanol–acetic acid (90:10, v/v). Typical HPLC chromatograms with 10.0 ng mL⁻¹ RB sample are presented in Fig. 5b. These show the obvious presence of the chili powder matrix background. The chromatogram for the original sample extracted using a single GO/SiO₂-MISPE column showed an obvious peak of RB, while the peaks corresponding to impurities were weak (Fig. 5c). The results illustrated in Fig. 5d were obtained using chip-based array columns and show a very apparent peak of RB; other compounds in the real samples were essentially negligible. According to the chromatographic peak area and standard curve, the final concentration was over 110 times that of the original sample, and extraction on the chip-based array columns eliminated potential sources of interference in the chili powder. This proved that the sensitivity was effectively increased using this method. Evidently, the enrichment and impurity removal effects of the chip-based array columns were higher than those of the single column.

3.6. Comparison of the MISPE columns and chip-based MISPE array columns

To clarify the difference in performance between MISPE columns and chip-based MISPE array columns, 12 RB MISPE columns of 3.3 cm long, fabricated at different times, were evaluated. Recovery was investigated by loading 200 μL of 5.0 μg mL⁻¹ RB standard solution. The recoveries of MISPE columns ranged from 87.8% to 92.4%, and the RSD was 1.3%. In addition, the 12 MISPE columns

Table 1
Recoveries of RB spiked in chili powder.

Analyte	Concentration (μg mL ⁻¹)	Recoveries (%)	RSD (%)	
			Inter-day repeatability (n = 6)	Intra-day repeatability (n = 3)
RB	0.01	88.4	2.5	4.0
	0.1	83.7	2.9	3.6
	1.0	85.6	3.1	3.2

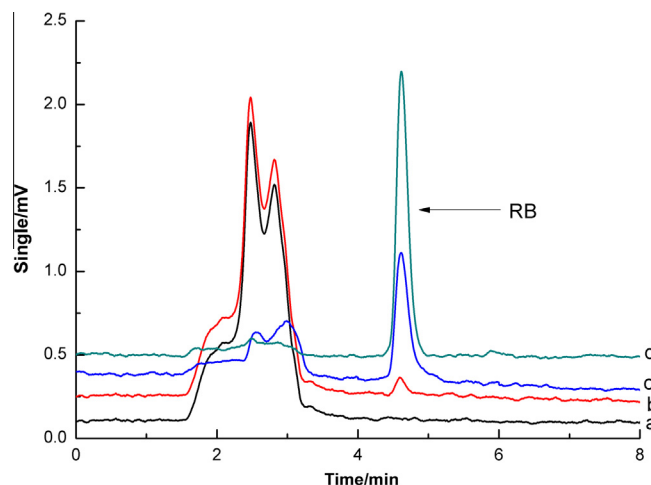


Fig. 5. Illustrative chromatograms for the sample enrichment and impurities removal: (a) blank sample without RB; (b) 10.0 ng mL⁻¹ RB sample before loaded onto the column; (c) 10.0 ng mL⁻¹ RB sample after loaded onto single column. (d) 10.0 ng mL⁻¹ RB sample after loaded onto the chip-based MISPE array columns.

of 3.3 cm long were embedded in 3 chips and 1.0 mL of 5.0 µg mL⁻¹ RB standard solution was loaded on the chips. The recoveries for the three chip-based array MISPE columns were 82.8% to 88.4%, and the RSD was 3.4%. Dead volume in the two ports of the chip resulted in slightly lower extraction recoveries for the chip-based array columns than MIPSE columns. The combined chip with four columns of GO/SiO₂-MISPE was beneficial for better enrichment capacity and improved selection efficiency. Additionally, the prepared columns and chips can be reused at least 30 times with similar extraction efficiency.

4. Conclusions

A novel PDMS/glass chip integrated with RB-imprinted monolithic capillary array columns was prepared using GO/SiO₂ as the support matrix. The chip-based array columns were used to effectively extract and enrich RB from chili powder, and the experimental conditions were optimized, including the T:M:C ratio, porogen type, and elution conditions. The GO/SiO₂-MISPE columns were characterized by SEM and FT-IR and the IF reached 7.07, which indicated a higher adsorption capacity, selectivity, and affinity than conventional MISPE columns, as well as improved enrichment and impurity removal. The proposed method is promising for RB analysis in real chili powder samples with a LOD of 0.40 ng g⁻¹ and enrichment factor of more than 110-fold owing to the high recovery, stability, and sensitivity.

Acknowledgements

The authors gratefully acknowledge financial support from the National Natural Science Foundation of China (NSFC, Grant No. 21005021), Natural Science Foundation of Guangdong Province (No. 2016A030313740) and Guangdong Provincial Science and Technology Project (No. 2013B04040).

Appendix A. Supplementary data

Supplementary data associated with this article can be found, in the online version, at <http://dx.doi.org/10.1016/j.foodchem.2016.07.124>.

References

- Castro López, M., Cela Pérez, M. C., Dopico García, M. S., López Vilarino, J. M., González Rodríguez, M. V., & Barral Losada, L. F. (2012). Preparation, evaluation and characterization of quercetin-molecularly imprinted polymer for preconcentration and clean-up of catechins. *Analytica Chimica Acta*, 721, 68–78.
- Duan, H. M., Li, L. L., Wang, X. J., Wang, Y. H., Li, J. B., & Luo, C. N. (2015). A sensitive and selective chemiluminescence sensor for the determination of dopamine based on silanized magnetic graphene oxide-molecularly imprinted polymer. *Spectrochimica Acta Part A-Molecular and Biomolecular Spectroscopy*, 139, 374–379.
- Duffy, D. C., McDonald, J. C., Seubler, O. J. A., & Whitesides, G. M. (1998). Rapid prototyping of microfluidic systems in poly(dimethylsiloxane). *Analytical Chemistry*, 70, 4974–4984.
- Farid, M. M., Goudini, L., Piri, F., Zamani, A., & Saadati, F. (2016). Molecular imprinting method for fabricating novel glucose sensor: Polyvinyl acetate electrode reinforced by MnO₂/CuO loaded on graphene oxide nanoparticles. *Food Chemistry*, 194, 61–67.
- Gao, N., Chen, Y. J., & Jiang, J. (2013). Ag@Fe₂O₃-GO nano composites prepared by a phase transfer method with long-term antibacterial property. *ACS Applied Materials & Interfaces*, 5, 11307–11314.
- Hummers, W. S., & Offeman, R. E. (1958). Preparation of graphitic oxide. *Journal of the American Chemical Society*, 80, 1339.
- Jackson, E., Ferrari, M., Cuestas-Ayllon, C., Fernandez-Pacheco, R., Perez-Carvajal, J., Martinez de la, F. J., et al. (2015). Protein templated biomimetic silica nanoparticles. *Langmuir*, 31, 3687–3695.
- Lata, K., Sharma, R., Naik, L., Rajput, Y. S., & Mann, B. (2015). Synthesis and application of cephalixin imprinted polymer for solid phase extraction in milk. *Food Chemistry*, 184, 176–182.
- Li, Y., Qi, L., & Ma, H. (2013). Preparation of porous polymer monolithic column using functionalized graphene oxide as a functional crosslinker for high performance liquid chromatography separation of small molecules. *Analyst*, 138, 5470–5478.
- Liu, H. L., Fang, G. Z., Zhu, H. D., Li, C. M., Liu, C. C., & Wang, S. (2013). A novel ionic liquid stabilized molecularly imprinted optosensing material based on quantum dots and graphene oxide for specific recognition of vitamin E. *Biosensors & Bioelectronics*, 47, 127–132.
- Longmire, M. R., Ogawa, M., Hama, Y., Kosaka, N., Regino, C. A. S., Choyke, P. L., et al. (2008). Determination of optimal rhodamine fluorophore for in vivo optical imaging. *Bioconjugate Chemistry*, 19, 1735–1742.
- Meng, J., Zhang, W., Bao, T., & Chen, Z. (2015). Novel molecularly imprinted magnetic nano particles for the selective extraction of protoberberine alkaloids in herbs and rat plasma. *Journal of Separation Science*, 38, 2117–2125.
- Milanova, D., Chambers, R. D., Bahga, S. S., & Santiago, J. G. (2011). Electrophoretic mobility measurements of fluorescent dyes using on-chip capillary electrophoresis. *Electrophoresis*, 32, 3286–3294.
- Ning, F. J., Peng, H. L., Li, J. H., Chen, L. X., & Xiong, H. (2014). Molecularly imprinted polymer on magnetic graphene oxide for fast and selective extraction of 17β-estradiol. *Journal of Agricultural and Food Chemistry*, 62, 7436–7443.
- Olof, R., Kristina, S., John, H., Pradip, P., & Oliver, B. (2014). Food analyses using molecularly imprinted polymers. *Journal of Agricultural and Food Chemistry*, 62, 7436–7443.
- Tatebe, C., Zhong, X., Ohtsuki, T., Kubota, H., Sato, K., & Akiyama, H. (2014). A simple and rapid chromatographic method to determine unauthorized basic colorants (rhodamine B, auramine O, and pararosaniline) in processed foods. *International Journal of Food Sciences and Nutrition*, 2, 547–556.
- Unsal, Y. E., Soylak, M., & Tuzen, M. (2014). Spectrophotometric detection of rhodamine B after separation-enrichment by using multi-walled carbon nanotubes. *Journal of AOAC International*, 97, 1459–1462.
- Wang, S., Xu, Z., Fang, G., Zhang, Y., & He, J. (2008). Separation and determination of estrone in environmental and drinking water using molecularly imprinted solid phase extraction coupled with HPLC. *Journal of Separation Science*, 31, 1181–1188.
- Xiao, W., Zhang, Y., & Liu, B. (2015). Raspberry like SiO₂@reduced graphene oxide@AgNP composite microspheres with high aqueous dispersity and excellent catalytic activity. *ACS Applied Materials & Interfaces*, 7, 6041–6046.
- Yuan, K. S., Wang, J. Z., Zhai, H. Y., Chen, Z. G., Huang, L., & Su, Z. H. (2015). Sensitive determination of rose bengal in brown sugar by a molecularly imprinted solid-phase extraction monolithic capillary column coupled with capillary electrophoresis. *Analytical Methods*, 7, 8297–8303.
- Zeng, Y. B., Zhou, Y., Kong, L., Zhou, T. S., & Shi, G. Y. (2015). A novel composite of SiO₂-coated graphene oxide and molecularly imprinted polymers for electrochemical sensing dopamine. *Biosensors & Bioelectronics*, 45, 25–33.
- Zhai, H. Y., Li, J. M., Chen, Z. G., Su, Z. H., Liu, Z. P., & Yu, X. (2014). A glass/PDMS electrophoresis microchip embedded with molecular imprinting SPE monolith for contactless conductivity detection. *Microchemical Journal*, 114, 223–228.
- Zhai, H. Y., Su, Z. H., Chen, Z. G., Liu, Z. P., Yuan, K. S., & Huang, L. (2015). Molecularly imprinted coated graphene oxide solid-phase extraction monolithic capillary column for selective extraction and sensitive determination of phloxine B in coffee bean. *Analytica Chimica Acta*, 865, 16–21.
- Zhang, M., Zeng, J., Wang, Y., & Chen, X. (2013). Developments and trends of molecularly imprinted solid-phase microextraction. *Journal of Chromatographic Science*, 51, 577–586.